A case study of the sizing and optimisation of an energy pile foundation (Rosborg, Denmark)

Alberdi-Pagola, Maria; Poulsen, Søren Erbs; Jensen, Rasmus Lund; Madsen, Søren

Published in:
Renewable Energy

DOI (link to publication from Publisher):
10.1016/j.renene.2018.07.100

Publication date:
2020

Document Version
Accepted author manuscript, peer reviewed version

Renewable Energy xxx (2018) 1–12

Contents lists available at ScienceDirect

Renewable Energy

journal homepage: www.elsevier.com/locate/renene

A case study of the sizing and optimisation of an energy pile foundation (Rosborg, Denmark)

Maria Alberdi-Pagola [a, *], Søren Erbs Poulsen [b], Rasmus Lund Jensen [a], Søren Madsen [c]

[a] Department of Civil Engineering, Aalborg University, Denmark
[b] VIA Building, Energy & Environment, VIA University College, Denmark
[c] COWI A/S, Denmark

ARTICLE INFO

Article history:
Received 31 May 2018
Received in revised form
17 July 2018
Accepted 19 July 2018
Available online xxx

Keywords:
Foundation pile heat exchanger
Energy pile
Interaction
Semi-empirical model
Case study
Optimisation

ABSTRACT

This paper applies previously validated multiple pile g-functions, for estimating operational average fluid temperatures in an actual energy pile foundation in Rosborg, Denmark. We find that the multiple pile g-functions yield fluid temperatures similar to what is observed, at minimal computational cost. The temperature model is then utilised in an optimisation algorithm that yields the minimum number of energy piles required by simultaneously maximising the pile spacing and taking into consideration the thermal load of the building. The optimisation shows that the thermal needs of the building can be fully supplied by 148 rearranged energy piles, instead of the current 219. The optimisation tool is also applied to a full-factorial design sweep which shows a large sensitivity of the number of energy piles on the thermal conductivity of the ground.

1. Introduction

Ground source heat pump (GSHP) systems produce renewable thermal energy that offer high levels of efficiency for space heating and cooling [1]. GSHP systems have a significant impact on the direct use of geothermal energy, accounting for 70% of the world-wide installed capacity [2].

Foundation pile heat exchangers (henceforth referred to as energy piles) are an alternative to borehole heat exchangers (BHE) when deep foundation is required in a building [3]. Fig. 1 presents an example of precast energy piles.

Relative to BHEs, energy piles have lower initial costs [4,5], their potential to minimise the overall environmental impact of a structure has been demonstrated [6] and their contribution towards zero energy buildings has been suggested too [7].

The thermal dimensioning of energy pile foundations is typically addressed by methods developed for borehole heat exchangers which are implemented in commercial software such as GLHEPro [8], EED [9], LoopLink PRO [10] or GLD [11]. Optimisation strategies for sizing GSHP systems have also been reported in the literature. De Paly et al. [12] minimise the soil temperature change over time by adjusting the individual heat extraction rate in each borehole; Beck et al. [13] adjust the position of each borehole individually and Maragna [14] uses multi objective optimisation to find a balance between the borehole field configuration and economic parameters.

The thermal design of energy pile foundations should follow a similar approach, in an attempt to balance performance and costs: the number of pile heat exchangers must cover the thermal requirements of the building without compromising the sustainability of the installation and without incurring excessive expenses. However, in energy foundations, unlike borehole heat exchanger fields, the available area, the length and position of the pile heat exchanger are determined by the structural requirements which renders optimisation tools that allows rearrangement of the heat exchanger field improper [15].

Despite the large potential in the field of energy foundations, their implementation is limited. Some of the causes for the low spread are the low cost of other energy sources - such as district heating [16], natural gas grid or fossil fuels [1] - the lack of financial incentives [1], the higher cost associated to the additional pipe works opposed to the standard foundations [5], as illustrated in

* Corresponding author. Department of Civil Engineering, Thomas Manns Vej 23, DK-9220 Aalborg Ø, Denmark.
E-mail address: mapa@civil.aau.dk (M. Alberdi-Pagola).

https://doi.org/10.1016/j.renene.2018.07.100
0960-1481/

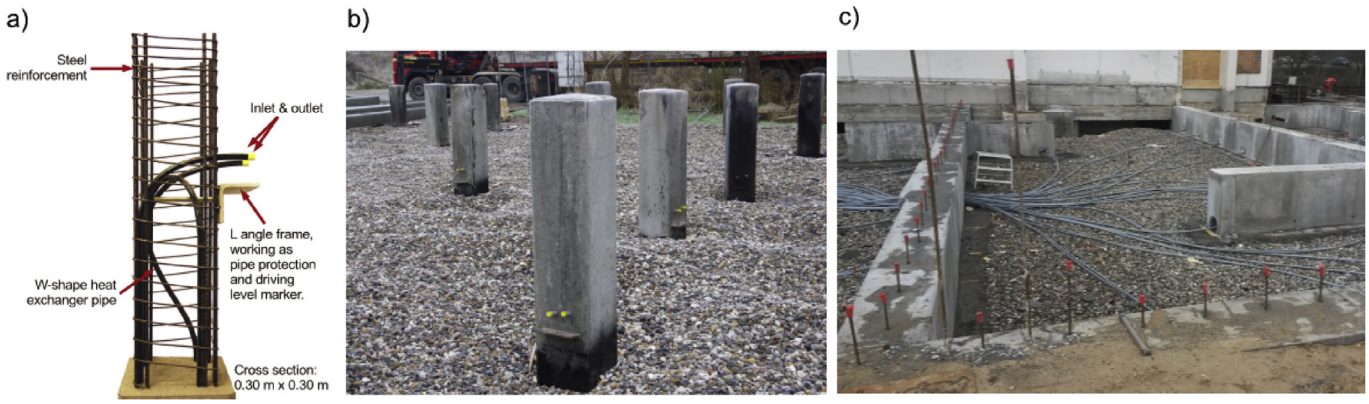

Fig. 1. a) Demonstration model of the precast pile heat exchanger with built in geothermal pipes. b) Pile heat exchanger field after driving. c) Pipe work.

Fig. 1, and the lack of information regarding the technology in early stage decision making. Specific tools and guidelines that account for the particularities of energy foundations would ease their utilisation.

PILESIM [17] is an experimentally validated commercial software for energy piles, however it does not take irregular patterns into consideration. Makasis et al. [18] uses machine learning to find the maximum energy that can be provided by a specified energy pile foundation, yet the method has not yet been applied to irregular pile patterns.

Foundation piles may be placed in irregular grids, since their position is subject to the mechanical load distribution received from the building. Precast piles are thinner and, usually, shorter than in-situ piles and, therefore, under comparable conditions, a higher amount of precast piles is needed to compensate their smaller size, reducing the pile spacing. Precast piles are occasionally placed irregularly in clusters, from singles to fours, spaced less than 1 m apart. The small pile spacing causes significant thermal interaction between neighbouring energy piles. This increases the required number of piles and entails higher costs during construction and operation. Hence, it appears reasonable to equip only a subset of the foundation piles as ground source heat exchangers so long the foundation is able to meet the thermal requirements of the building [19]. This trade-off leads to an optimisation problem in which the number of energy piles and which piles to pick as ground source heat exchangers are constrained by a need to maintain long term sustainable ground temperatures and to meet the thermal requirements of the building.

Previous research on precast pile heat exchangers [20] has shown that semi-empirical multiple pile g-functions yield reliable estimates of fluid temperatures for relatively small, irregular pile arrays. This paper continues the work presented in Ref. [20] and aims to analyse the applicability of the multiple pile g-functions in a case study of Rosborg Gymnasium, Denmark, which is founded on energy piles and to propose an optimisation strategy based on the desirability function approach [21] to minimise the number of energy piles.

2. Methods

The fluid temperatures to the heat pump for the energy pile foundation in Rosborg is modelled with semi-empirical g-functions that are described briefly in the following (we refer the reader to [20,22] for additional information). The optimisation procedure is then described.

2.1. Multiple pile g-functions

The average fluid temperature T_f [°C] for a group of pile heat exchangers is:

$$T_f = T_0 + \frac{q}{2\pi\lambda_s} G_g + qR_cG_c + qR_{pipe} \quad (1)$$

where T_0 [°C] is the undisturbed soil temperature, q [W/m] is the heat transfer rate per metre length of energy pile, λ_s [W/m/K] is the thermal conductivity of the soil, G_g is the multiple pile g-function for the ground temperature response, R_c [K·m/W] is the steady state concrete thermal resistance, G_c is the concrete G-function for the transient response of the pile and R_{pipe} [K·m/W] is the thermal resistance of the pipes.

G-functions are dimensionless curves of the change in temperature in the ground over time from applying a thermal load on the pile [23]. The pile g-functions in this study are derived from 3D temperature modelling of single energy piles for different pile length to diameter ratios (aspect ratio), which yield pile and soil temperatures at specified radial distances.

G_g depends on the aspect ratio of the pile heat exchanger, the number of piles and the pile spacing. To account for the interaction between piles, the multiple pile g-function G_g is calculated by temporal and spatial superposition of single pile g-function temperatures. G_c and R_c depend on the position of the pipes and the ratio between the thermal conductivity of the concrete and the soil. R_{pipe} depends on the thermal properties and flow rate of the heat carrier fluid and the thermal conductivity of the pipe. The dimensionless temperatures and curves are fitted with polynomials, to ease implementation. A detailed explanation of the method, comprising the dimensionless type curves and the coefficients for G_g, G_c and R_c, is given in Refs. [20,22] and a summary of the equations and coefficients applied in this study is provided in Appendix A.

2.2. Optimisation of pile heat exchanger design

The geometrical arrangement of foundation piles is determined solely by the structural requirements of the building. However, it is important that the spatial arrangement of the energy piles is as uniform as possible to avoid significant local changes in the soil temperature, which potentially have implications for the structural integrity of the piles, and ensure homogeneous thermal settlements or uplifts, if any [24]. Once an energy pile pattern is chosen from the predefined grid of foundation piles, corresponding fluid temperatures are estimated with the multiple pile g-functions. The

Please cite this article in press as: M. Alberdi-Pagola, et al., A case study of the sizing and optimisation of an energy pile foundation (Rosborg, Denmark), Renewable Energy (2018), https://doi.org/10.1016/j.renene.2018.07.100

energy pile pattern is then adjusted until the desired temperatures are achieved while honouring the thermal requirements of the building.

2.2.1. Optimisation of pile arrangement

The ideal way to place ground heat exchangers in a field is by minimising the influence between them which corresponds to maximising the pile spacing. To provide the energy pile arrangement that maximises the pile spacing, given the structural constraints, a constrained optimisation scheme is proposed. The scheme accepts as input the coordinates of the foundation piles, the number of required energy piles and a minimum initial pile spacing. The MATLAB "*patternsearch*" non-continuous subroutine [25] is utilised for determining the arrangement of the required energy piles, while maximising pile spacing. For every computation, the local optimisation algorithm distributes n_p piles by maximising their spacing. Therefore, the optimiser finds the maximum pile spacing that can accommodate n_p piles in the provided grid, i.e., leading to a uniform pile distribution covering as much free space as possible.

Fig. 2 shows an example of a foundation pattern with 11 piles of which 7 are aimed to be energy piles. An initial guess for the desired energy pile spacing is also chosen, e.g., 4 m. Now, the optimisation scheme attempts to find the best distribution for the required 7 energy piles. However, due to the predefined position of the piles, it is not possible to pick 7 energy piles because the condition to keep a 4-m pile spacing (dotted grey line) cannot be fulfilled. Hence, the optimisation scheme reduces the pile spacing to 3 m (solid grey line) and tries again to select among the existing piles, successfully now, the ones that should be equipped as energy piles. The prevailing condition is to keep the number of energy piles initially imposed and the algorithm will adapt the energy pile spacing, to keep it as high as possible, given the geometric restrictions.

2.2.2. Desirability function approach

The multiple pile g-function model is applied to the pile arrangement determined by the optimisation scheme outlined in the previous subsection (2.2.1) to yield average fluid temperatures in the ground loop (Equation (1)). Now, the optimum number of pile heat exchangers required to supply a given building demand is determined by maximising a so-called desirability function. The

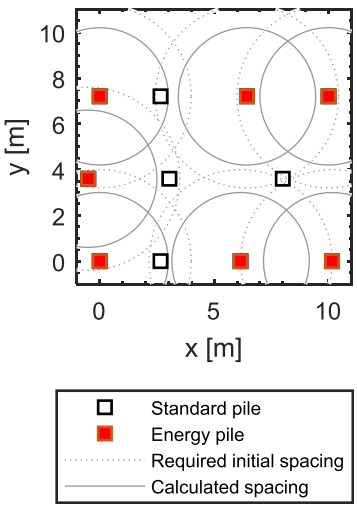

Fig. 2. Optimum arrangement of 7 energy piles in a foundation with 11 foundation piles.

desirability function approach [21], also described in Refs. [26,27], is used for optimisation of multiple response processes by assigning a desirability function $d_i(Y_i)$ value between 0 and 1 to each response $Y_i(x)$, where $d_i(Y_i) = 0$ and $d_i(Y_i) = 1$ represent unacceptable and ideal responses, respectively. The individual desirabilities are combined using the geometric mean, to give the overall desirability D (hereon the notation used in Ref. [27] is adopted):

$$D = (d_1(Y_1)d_2(Y_2)\ldots d_k(Y_k))^{1/k} \tag{2}$$

where k is the number of responses. Clearly, if any response Y_i is completely undesirable, i.e., $d_i(Y_i) = 0$, then the overall desirability is zero.

Different desirability functions $d_i(Y_i)$ are defined, depending on whether a response Y_i is to be maximised, minimised or assigned a target value. Let define L_i, U_i and T_i as lower, upper and target values, respectively. According to this, the desired response Y_i needs to fall within $L_i \le T_i \le U_i$.

When a specific value needs to be assigned to a response (a.k.a. target is best), its desirability functions is defined as:

$$d_i(Y_i) = \begin{cases} 0 & \text{if} \quad Y_i(x) < L_i \\ \left(\dfrac{Y_i(x) - L_i}{T_i - L_i}\right)^s & \text{if} \quad L_i \le Y_i(x) \le T_i \\ \left(\dfrac{Y_i(x) - U_i}{T_i - U_i}\right)^t & \text{if} \quad T_i \le Y_i(x) \le U_i \\ 0 & \text{if} \quad Y_i(x) > U_i \end{cases} \tag{3}$$

where s and t determine the importance to hit the target value. When $s = t = 1$, the desirability function increases linearly towards the target value T_i.

When a response needs to be maximised, its desirability function is defined as:

$$d_i(Y_i) = \begin{cases} 0 & \text{if} \quad Y_i(x) < L_i \\ \left(\dfrac{Y_i(x) - L_i}{T_i - L_i}\right)^s & \text{if} \quad L_i \le Y_i(x) \le T_i \\ 1 & \text{if} \quad Y_i(x) > T_i \end{cases} \tag{4}$$

where T_i is understood as a large enough value for the response.

Lastly, when a response needs to be minimised, its desirability function is defined as:

$$d_i(Y_i) = \begin{cases} 1 & \text{if} \quad Y_i(x) < T_i \\ \left(\dfrac{Y_i(x) - U_i}{T_i - U_i}\right)^s & \text{if} \quad T_i \le Y_i(x) \le U_i \\ 0 & \text{if} \quad Y_i(x) > U_i \end{cases} \tag{5}$$

where T_i is understood as a small enough value for the response.

The desirability approach penalises the values that differ from the target values or admissible limits and allows the assignment of weights to the different responses. In this study, the desirability function is defined by adjusting three responses simultaneously:

i) The number of energy piles, which needs to be minimised. It is limited between 1 (ideally, a single pile would need to be an energy pile) and the total number of foundation piles, i.e., thermally activating all the standard piles.
ii) The return temperature to the ground loop. The minimum allowed temperature in the ground loop must exceed 0 °C [28], with a target value of 2 °C ("target is best"), to minimise

Please cite this article in press as: M. Alberdi-Pagola, et al., A case study of the sizing and optimisation of an energy pile foundation (Rosborg, Denmark), Renewable Energy (2018), https://doi.org/10.1016/j.renene.2018.07.100

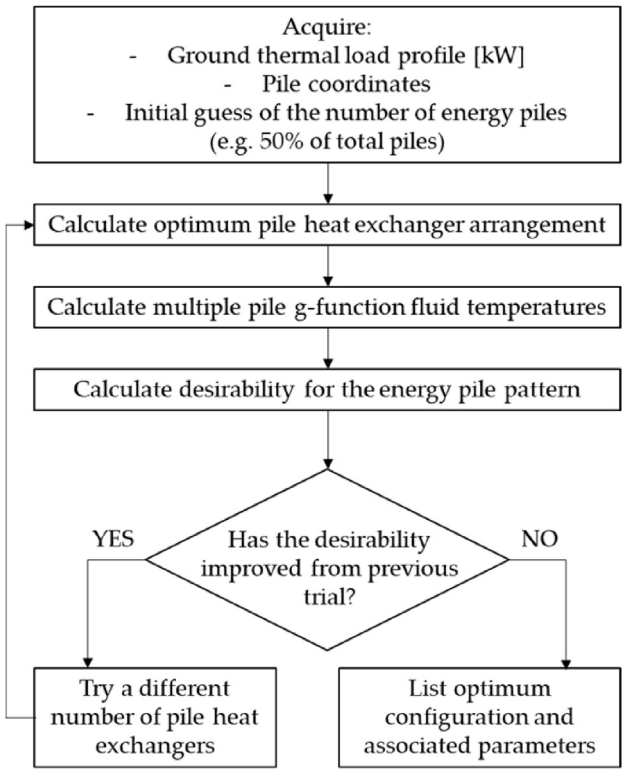

Fig. 3. Workflow for obtaining the optimum number and arrangement of energy piles.

thermal effects on the mechanical response of the pile. The upper limit is set to 20 °C.

iii) The long-term average fluid temperature must be as close as possible to the initial soil temperature to ensure stable performance of the heat pump over time and to mitigate the environmental impact of the system ("target is best").

The three responses have been assigned equal weights. The practical implementation of the method is divided into the steps shown in Fig. 3. Once an optimum configuration for n_p piles is determined, the global optimisation algorithm calculates the corresponding fluid temperatures. In the proposed scheme, the energy pile pattern is updated until the temperature requirements defined in the desirability function are satisfied. The optimisation scheme is also applied to a full-factorial design sweep of the case study where the thermal conductivity of the soil λ_s [W/m/K] and the thermal load Q [kW] are varied to analyse the sensitivity of the energy foundation to varying conditions.

3. Case study

The southern extension of Rosborg Gymnasium high school in Vejle, Denmark, is founded on 269 piles, 219 of which are energy piles (Fig. 4). All 269 piles were scheduled to serve as energy piles, however, 50 piles were cut as the desired foundation depth could not be reached by hammering. The driven, quadratic cross section (30 cm by 30 cm), precast 15 m energy piles are fitted with W-shaped heat exchanger piping (Fig. 1). In Denmark, 90% of the piles are precast [29] and between 85 and 90% of the production is addressed to the building industry [30]. Standard dimensions are square sections with dimension from 25 cm to 45 cm (Fig. 1).

The ground source heat pump system has supplied the space heating need of the 3950 m^2 living area since autumn 2012 which amounts to approximately 135 MWh/year. The system is capable of supplying free cooling to the southern rooms (approx. 900 m^2), however, this option is rarely used and the cooling amounts to just 2 MWh/year (Fig. 5). The ground thermal load is also provided in Fig. 5 (81 MWh/year).

The pile heat exchangers are connected in parallel. The ground loop utilises a 20% ethylene glycol-based water solution as heat carrier fluid. The heat pump consists of a water-to-water unit with a heating capacity of 200 kW and two compressors. The heat pump charges a water accumulation tank (55 °C) from which a traditional radiator-based heating system is supplied. The district heating network serves as an auxiliary heating system. Free cooling uses ventilation fan-coils coupled to the ground loop.

The foundation is situated 70 cm below terrain, just below the primary groundwater table. The foundation piles are placed in glacial sand and gravel sediments situated at 5–6 m below terrain, topped by postglacial organic clay [31–33]. Fig. 6 shows the density, thermal conductivity and volumetric heat capacity profiles for the site. The case study is further described in Refs. [31,32].

3.1. Data processing

The inlet and outlet temperature time series as well as the total

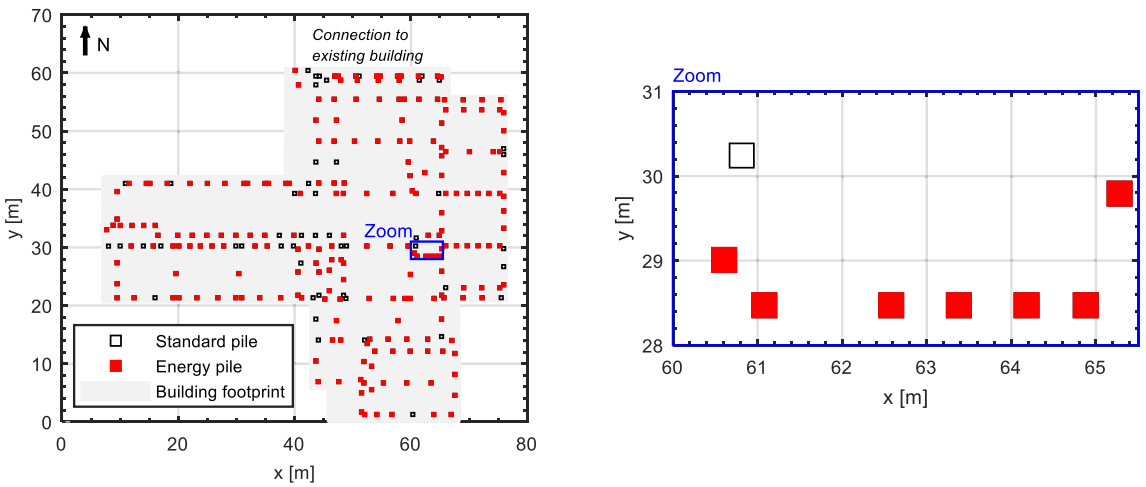

Fig. 4. Top view of foundation pattern of the case study. a) Overview; b) Zoom to a high pile density area. The legend is common for both subplots.

Please cite this article in press as: M. Alberdi-Pagola, et al., A case study of the sizing and optimisation of an energy pile foundation (Rosborg, Denmark), Renewable Energy (2018), https://doi.org/10.1016/j.renene.2018.07.100

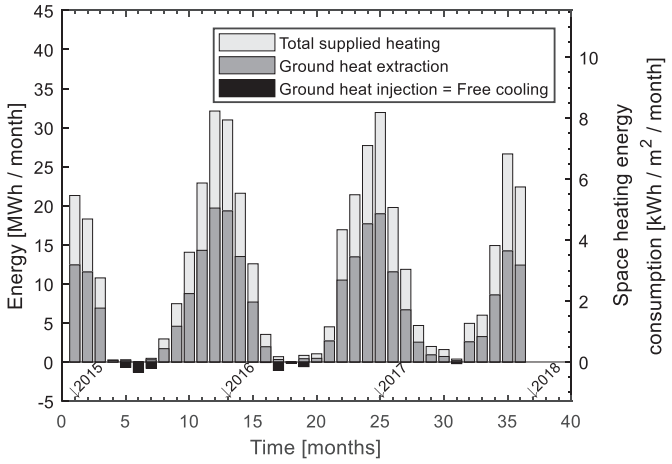

Fig. 5. Supplied heating and cooling at Rosborg Gymnasium, Denmark.

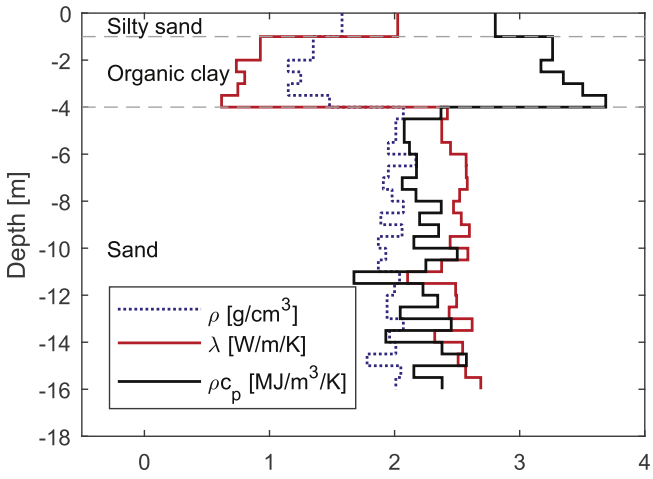

Fig. 6. Density ρ [g/cm^3], thermal conductivity λ [W/m/K] and volumetric heat capacity ρc_p [MJ/m^3/K] profile at the Rosborg test site, after [33]. Depth is relative to the ground surface.

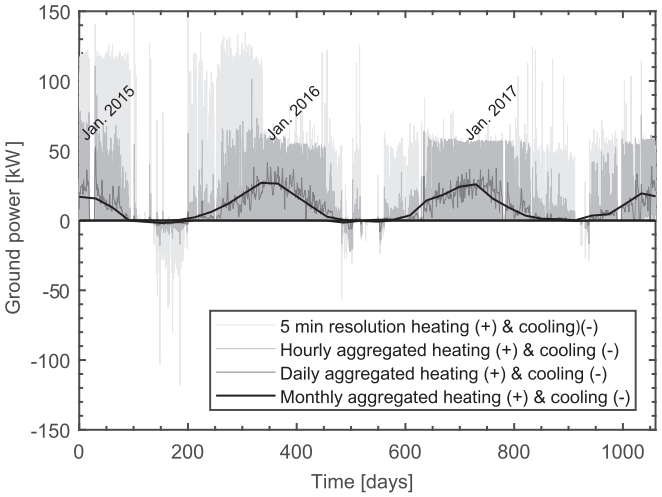

Fig. 7. Measured ground thermal power (2015–2017) at 5-min resolution and hourly, daily and monthly aggregated powers, respectively.

Table 1
Parameters for the case study.

Undisturbed soil temperature	T_0 [°C]	10.20
Thermal conductivity of soil	λ_s [W/m/K]	2.21
Volumetric heat capacity of soil[a]	ρc_{ps} [MJ/m^3/K]	2.47
Thermal conductivity of concrete	λ_c [W/m/K]	3.05
Volumetric heat capacity of concrete	ρc_{pc} [MJ/m^3/K]	2.37
Thermal conductivity of fluid	λ_f [W/m/K]	0.54
Volumetric heat capacity of fluid	ρc_{pf} [MJ/m^3/K]	4.01
Density of fluid	ρ_f [kg/m^3]	1048
Dynamic viscosity heat carrier fluid	μ_f [Pa·s]	0.002
Thermal conductivity of pipe	λ_p [W/m/K]	0.42
Total flow in ground loop	f_{total} [m^3/s]	0.0083
Number of pile heat exchangers	n_p [−]	219
Circulating flow per pile	f [m^3/s]	$3.39 \cdot 10^{-5}$
Pile active length	L [m]	15
Cross section size	S [m]	0.30 × 0.30
Energy pile aspect ratio	AR [−]	39
Number of pipes in cross section	n [−]	4
Pipe outer diameter	$Ø_{out}$ [m]	0.020
Pipe inner diameter	$Ø_{in}$ [m]	0.016

[a] Layer thickness-weighted arithmetic mean.

flow rate and the energy to/from the ground loop have been extracted from the building control and monitoring system. The raw data consist of 5-min averages recorded between 2015 and 2017 (Fig. 7). The measured thermal power and temperature time series are aggregated to hourly, daily and monthly averages (Fig. 7), ensuring conservation of energy.

For the computations, the operational data from 2015 and 2017 are extrapolated back in time to autumn 2012. During the first 3 years of operation, system start up implied reduced supplied heating and cooling and therefore, only 50% of the extrapolated demand is considered for the period 2012–2015. The studied energy pile foundation works mainly in heating mode, i.e., an unbalanced heat extraction over time is expected. In principle, this will lower long-term soil temperatures.

3.2. Model parameters

The model parameters utilised in the case study are listed in Table 1. Each of the parameters influences the overall thermal performance of the system and more about the implications can be learned in Refs. [34,35].

The undisturbed soil temperature T_0 is determined by field measurements prior to thermal response test (TRT) [33,36]. The thermal conductivities of the soil λ_s and the concrete λ_c are estimated from field TRT measurements, presented in Ref. [33]. The volumetric heat capacities of the soil ρc_{ps} and the concrete ρc_{pc}, are estimated from laboratory testing, also presented in Ref. [33]. The total flow circulating in the ground loop was recorded by the data acquisition and control system of the building [31]. The flow in each pile is the total flow divided by the number of energy piles. The fluid and pipe properties were obtained from manufacturer brochures [37,38].

4. Results and discussion

Firstly, the model is compared to operational data to demonstrate its validity. The optimisation method is then applied to the case study pile arrangement and the parameter sweep analyses the influence of variations in the soil thermal properties and building requirements on the required size of the energy foundation.

4.1. Model verification

To evaluate the predictive capabilities of the model, simulated average fluid temperatures have been compared to corresponding

Please cite this article in press as: M. Alberdi-Pagola, et al., A case study of the sizing and optimisation of an energy pile foundation (Rosborg, Denmark), Renewable Energy (2018), https://doi.org/10.1016/j.renene.2018.07.100

observations during the three years of collected data (Fig. 8).

The model reproduces the shape of the observed temperatures for heat extraction periods. When the heat removal from the ground dominates, the phenomena is mainly governed by conduction in the soil which is well captured by the model. The model reproduces the lowest temperatures which is critically important for ground source heat pump system.

The simulations diverge from the observations as the heating need decreases, i.e., in low activity or stand-by periods. In these stages, other factors, which are not considered by the model, begin to play a role: possible groundwater flow, heat island effect from the building, heat gains through the building standing on top of the foundation, seasonal surface temperature variations and indoor temperature sensors measuring on standing fluid in pipes.

4.1.1. Influence of load aggregation

To analyse the implication of using hourly, daily, weekly or monthly thermal loads, a comparison of computed temperatures with different levels of aggregation has been performed. The thermal load assumed in the comparison, corresponds to the average applied power in the period 2015–2017. Fig. 9 shows the residuals for the computed average fluid temperatures, relative to the hourly simulation.

When aggregated values are used, a loss of accuracy can be expected, as the temperatures calculated with the simplified thermal loads might not capture the peak temperatures. When a daily aggregation of the heat power is used, the most frequent difference with the hourly most critical temperatures is around 1 °C. Even though the occurrence of those critical low temperature does not extend over time, it is important to be aware of this fact during design and to consider the duration of the peak needs in the thermal load, as suggested in Ref. [9]. Unfortunately, this information is not available for the case study.

Weekly and monthly loads yield similar magnitude of residuals. Thus, as mentioned, a method to consider peak needs, their duration and permits the analysis of weekly or monthly loads will be beneficial since computation times can be shorten considerably, as shown in Table 2.

The accuracy and resolution of the simulations shall depend on the information available at every stage of the process and the resources, namely: feasibility study, dimensioning or operational optimisation. The higher the quality of the thermal profiles of the building, the more accurate will be the ground loop temperature predictions. It is important to refine the thermal loads as information is gathered so that the accuracy of the simulations can be improved.

The thermal response of the soil occurs on a timescale of hours. Previous research [20] has shown that the thermal disturbance at approximately 1 m distance from the pile begins after 1 day. Therefore, it is considered that the effect of the daily simplification on the model accuracy is minimal and, in the following, a daily thermal load will be analysed.

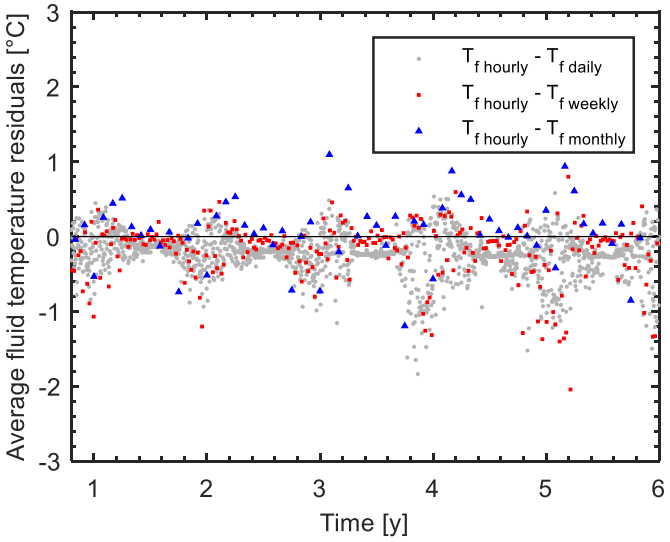

Fig. 9. Average fluid temperature T_f residuals for different time resolutions, relative to the hourly simulation.

Table 2
Computation times.

Simulated time	Resolution	Time-steps	Computation time [s]
25 years	Hourly	87600	450
	Daily	3650	95
	Weekly	522	2.75
	Monthly	120	0.88

4.2. Long-term ground temperature prediction

Fig. 10 shows the computed average fluid temperature following

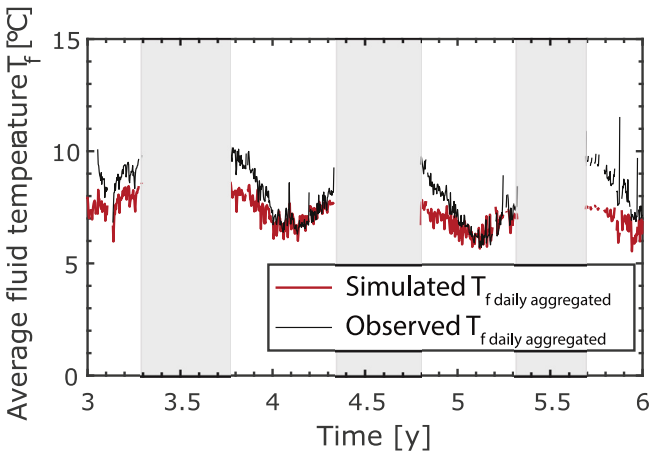

Fig. 8. Observed and modelled average fluid temperatures. The periods where heat extraction is non-existing are hidden.

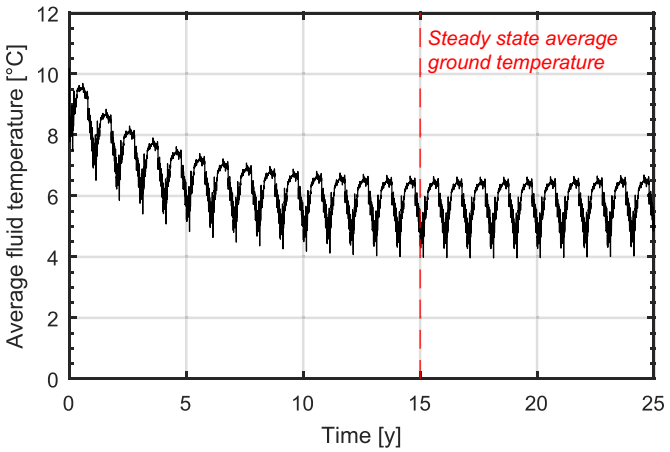

Fig. 10. Predicted long-term temperatures for Rosborg Gymnasium.

Please cite this article in press as: M. Alberdi-Pagola, et al., A case study of the sizing and optimisation of an energy pile foundation (Rosborg, Denmark), Renewable Energy (2018), https://doi.org/10.1016/j.renene.2018.07.100

25 years of operation, extrapolating existing heating and cooling loads. Computed temperatures are above 4 °C and steady-state average ground temperature conditions are established after 15 years of operation.

4.3. Optimisation of pile heat exchanger design

The dimensioning of the energy pile foundation in Rosborg was done conservatively by replacing all traditional foundation piles with energy piles. At this time, there were no guidelines nor tools available for dimensioning energy pile foundations. Consequently, the construction costs were potentially elevated from using an excess number of energy piles. In this section, we aim to properly dimension the energy pile foundation at Rosborg, by minimising the number of energy piles while still being able to supply the required heating and cooling loads and to ensure the long-term sustainability of ground temperatures.

The parameters for the optimisation are listed in Table 1. The Reynolds number of the ground loop flow rate is ca. 2500, indicating a transient regime between laminar and turbulent flow conditions. Previous research [20] has shown that there is not a significant reduction in the pipe thermal resistance when applying fully turbulent flow relative to high transient. 15-year simulations are carried out.

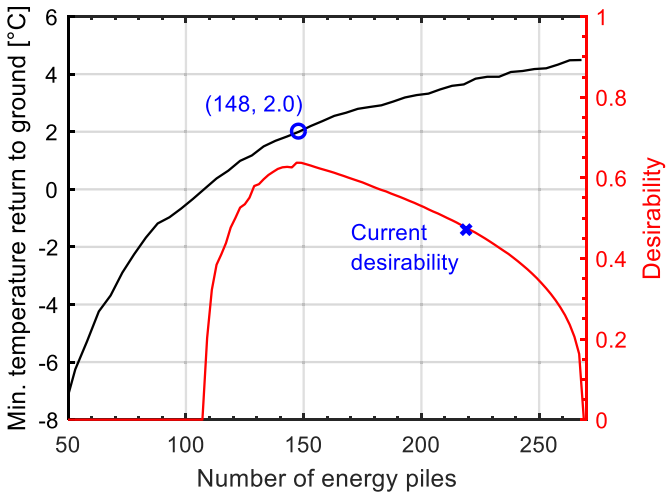

Fig. 11. Minimum return fluid temperature the ground loop and desirability for different numbers of energy piles.

Fig. 11 shows the dependence of the minimum temperature return to the ground loop and the desirability function on the number of energy piles. At least 105 energy piles are required for maintaining fluid temperatures above 0 °C. Since the desirability condition regarding sub-zero temperatures is not fulfilled, the overall desirability is zero. As the minimum fluid temperature increases, the desirability increases until the addition of additional energy piles is outweighed by the condition that ensures minimisation of the number of energy piles. Thus, as the number of energy piles increases, the desirability progressively falls to zero for the maximum number of energy piles.

The optimal arrangement, at which desirability is maximised, counts 148 energy piles, distributed as shown in Fig. 12. Fig. 12 also provides the optimum energy pile arrangements for 110 and 220 energy piles. The results imply that Rosborg Gymnasium can supply the current thermal demand with 32% less energy piles. The desirability of the current setup is also provided in Fig. 11. It falls practically on top of the desirability curve, meaning that when 219 piles are needed, the optimisation of the pile position gets harder and its influence is not significant. This is visible in Fig. 12c, where the higher amount of energy piles required, hardly leaves room for optimisation within the constraints. Therefore, the fluid temperatures that the model yields with the arrangement in Fig. 12c are similar to the ones obtained with the pile arrangement presented in Fig. 4.

Deciding upon the number of energy piles, depends, ultimately, on the engineer's judgement. Besides, the desirability function can be defined in an alternative way, assigning different weights or adding more responses, such as costs. Additional constraints and conditions modifies the shape of the desirability function, and, thus, potentially impacting the outcome of the optimisation.

4.4. Parametric study

The optimisation tool is applied in a full-factorial parameter sweep where the thermal conductivity of the soil λ_s [W/m/K] and the thermal load Q [kW] are varied to analyse the sensitivity of the performance of the energy pile foundation to varying conditions. The thermal conductivity of the soil varies from 1.0 to 3.5 W/m/K, based on typical soils in Denmark, whereas the thermal load requirements range between 0.5 and 1.5 times the current need of the building, i.e., between 40.5 MWh and 121.5 MWh of heat extraction per year. The remaining variables are kept as given in Table 1. The optimum pile arrangement is calculated for each parameter

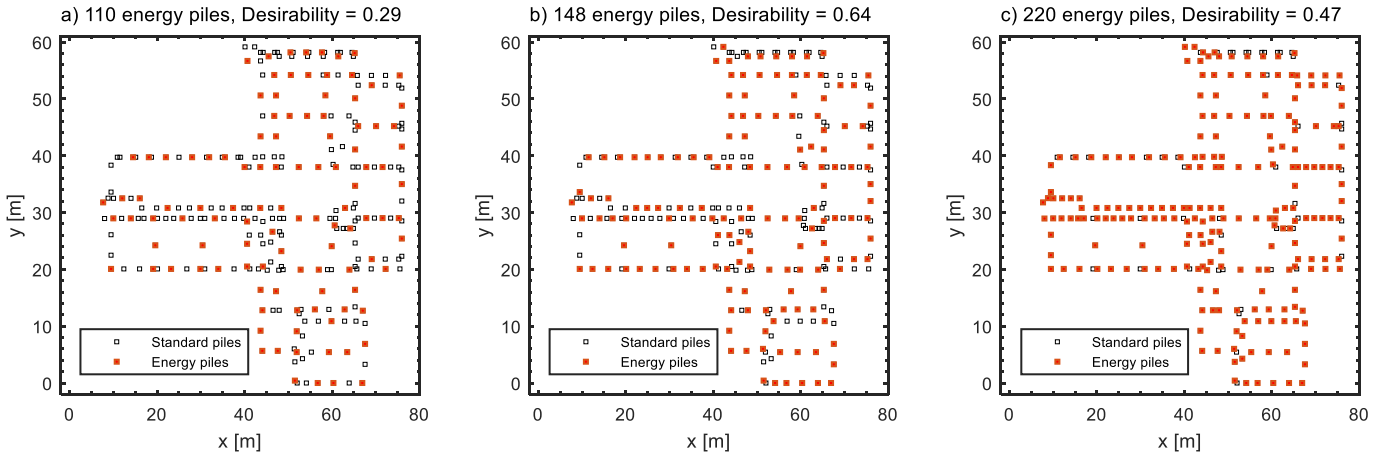

Fig. 12. Optimal location of energy piles for different desirabilities: 110, 148 and 220 pile heat exchangers for a), b) and c), respectively.

Please cite this article in press as: M. Alberdi-Pagola, et al., A case study of the sizing and optimisation of an energy pile foundation (Rosborg, Denmark), Renewable Energy (2018), https://doi.org/10.1016/j.renene.2018.07.100

combination (10^2) and contour plots of desirability, the number of required energy piles, the minimum temperature in the ground loop and the average fluid temperature are shown in Fig. 13.

The four subplots in Fig. 13 need to be read simultaneously. Fig. 13a shows the desirability contours for each parameter combination. The higher desirability contour lines approaching 1 on the left top part indicate that the three conditions that define the desirability are close to be simultaneously fulfilled. Meaning that, obviously, the higher the thermal conductivity of the soil and the lower the proportion of thermal load, the higher will be the desirability, the lower will be the required number of energy piles and the more satisfactory will be the temperature conditions.

The null desirability, highlighted in red, indicates an unacceptable boundary. This means that for high thermal load proportions (above 1.1) and low thermal conductivities of soil (below 1.6 W/m/K), even the maximum number of energy piles (269 in Fig. 13b) yields unacceptable minimum temperature of the return fluid to the ground (red lines in Fig. 13c).

Fig. 13c also indicates that acceptable minimum fluid temperatures are reached as the thermal conductivity of the soil increases. Fig. 13b shows a large sensitivity of the number of energy piles to the thermal conductivity of the ground. The thermal conductivity of the soil cannot be engineered and must be determined by appropriate field or laboratory measurements such as thermal response testing during the geotechnical investigations where piles are driven to assess the depth of the foundation [33].

It is common practice to design ground source heat pump installations to cover 80% of the heating load, given that peaks in demand are supplied by a complementary source [14]. Obtaining an accurate energy demand profile for a planned building is not always possible. In that case, parameter sweeps are useful for quantifying the uncertainty on the number of energy piles from having insufficient knowledge of the thermal load of the building. To that end, it must be stipulated, that obtaining accurate estimates of the heating and cooling requirements of a building in the planning phase is essential when applying the method presented in this paper.

5. Conclusions

We apply dimensionless temperature type curves (g-functions) and superposition techniques for estimating the fluid temperatures in energy pile foundations. The temperature model is applied in an optimisation scheme, based on the desirability function approach, in which the minimum number and arrangement of energy piles required for supplying the thermal needs of the building is estimated, while maintaining sustainable long-term temperatures.

The multiple pile g-functions yield reliable average fluid temperatures when compared to corresponding observed temperatures during heat extraction.

The optimisation tool shows that the number of pile heat exchangers needed for this case study could have been reduced by 32%.

The parameter sweep carried out provides practical design charts that support the dimensioning when the thermal load of the building and/or the soil thermal properties are uncertain.

The desirability function approach and the flexibility of the proposed method allow more conditions and features to be considered in future improvements, such as costs and

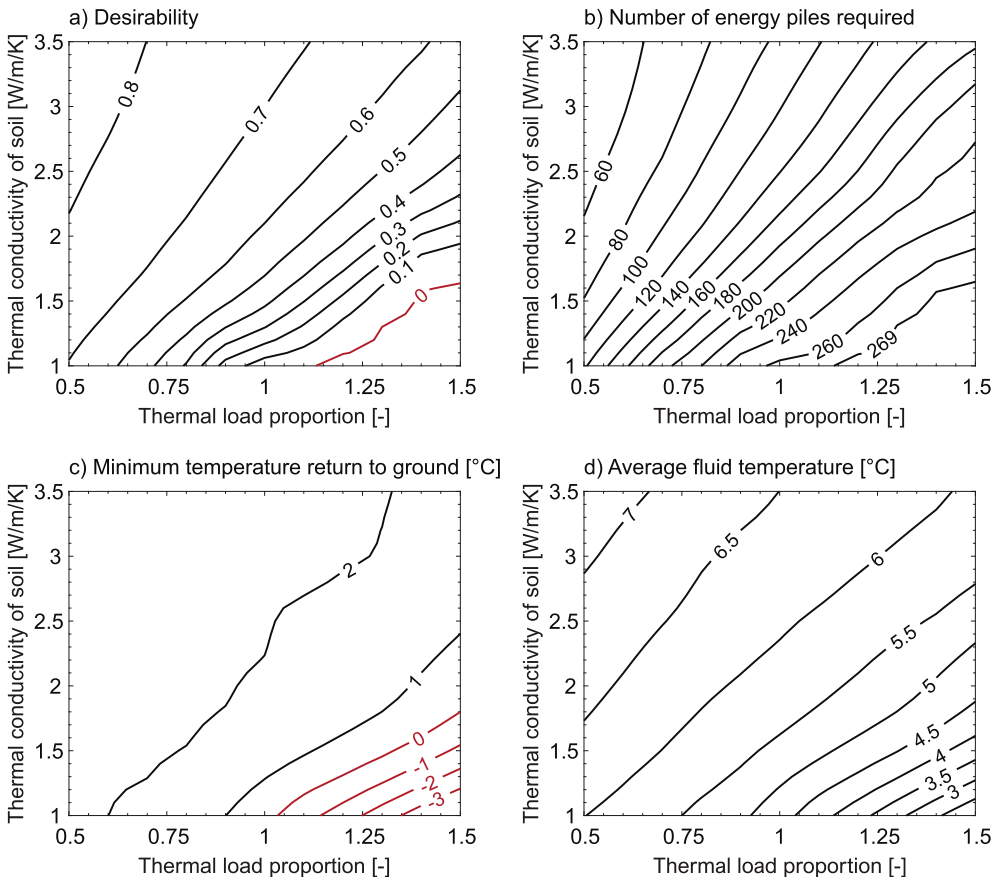

Fig. 13. a) Desirability, b) number of required energy piles, c) minimum temperature return to the ground loop and d) average fluid temperature, for the optimal pile arrangement.

Please cite this article in press as: M. Alberdi-Pagola, et al., A case study of the sizing and optimisation of an energy pile foundation (Rosborg, Denmark), Renewable Energy (2018), https://doi.org/10.1016/j.renene.2018.07.100

complementary energy sources. As such, the multiple pile g-function based temperature model combined with the proposed optimisation strategy offers a reliable basis for feasibility studies and for the dimensioning of energy pile foundations.

Acknowledgements

We kindly thank the following financial partners: Centrum Pæle A/S, INSERO Horsens, Denmark (project number 2014-084) and Innovationsfonden Denmark (project number 4135-00105A). We express our deep gratitude to Rosborg Gymnasium & HF for providing access to their installations and to Victor Marcos-Mesón for assistance with the MATLAB code.

Appendix A. Supplementary data

Supplementary data related to this article can be found at https://doi.org/10.1016/j.renene.2018.07.100.

Appendix B. Model development

As previously stated in Section 2, the average fluid temperature T_f [°C] for a group of pile heat exchangers is:

$$T_f = T_0 + \frac{q}{2\pi\lambda_s} G_g + qR_c G_c + qR_{pipe} \quad (A.1)$$

where T_0 [°C] is the undisturbed soil temperature, q [W/m] is the heat transfer rate per metre length of energy pile, λ_s [W/m/K] is the thermal conductivity of the soil, G_g is the multiple pile g-function for the ground temperature response, R_c [K·m/W] is the steady state concrete thermal resistance, G_c is the concrete G-function for the transient response of the pile and R_{pipe} [K·m/W] is the thermal resistance of the pipes. In the following, the equations for the various functions in Equation (A.1) are described. The following content is further described in Refs. [20,22] and, hence, this appendix comprises a summary.

$$q = f \cdot \rho c_{pf} \cdot \frac{(T_{in} - T_{out})}{n_p \cdot L} \quad (A.2)$$

$$T_f = \frac{(T_{in} + T_{out})}{2} \quad (A.3)$$

where f [m^3/s] is the circulating flow in the ground loop, ρc_{pf} [J/m^3/K] is the volumetric heat capacity of the heat carried fluid, T_{in} [°C] and T_{out} [°C] are the inlet and outlet temperatures in the ground loop, respectively, n_p is the number of energy piles comprising the energy foundation and L [m] is the active length per energy pile.

G-functions are dimensionless response factors that describe the change in temperature in the ground around a heat exchanger with time as a result of an applied thermal load q [23]. In this study, the normalised temperature changes Φ and time Fo are defined as:

$$\Phi = \frac{2\pi\lambda_s \Delta T}{q} \quad (A.4)$$

$$Fo = \frac{\alpha_s t}{r_b^2} \quad (A.5)$$

where ΔT [K] is the temperature change between the undisturbed soil temperature T_0 [°C] and the average pile wall temperature T_b [°C], α_s [m^2/s] is the thermal diffusivity, i.e., the ratio between the thermal conductivity λ_s [W/m/K] and the volumetric heat capacity of the soil ρc_{ps} [J/m^3/K], t [s] is the time and r_b [m] is the pile equivalent radius. The pile radius is the radius that provides an equivalent circumference to the square perimeter.

The pile g-functions in this study are derived from 3D temperature modelling of single energy piles for different pile length to diameter ratios (aspect ratio AR), as proposed in Refs. [19,39] and developed in Refs. [20,22], which yield pile and soil temperatures at specified radial distances. Fig. 14 shows the dimensionless temperature curves resulted from simulations of single energy piles with AR 30 and AR 45, at normalised distances $S/2r_b$.

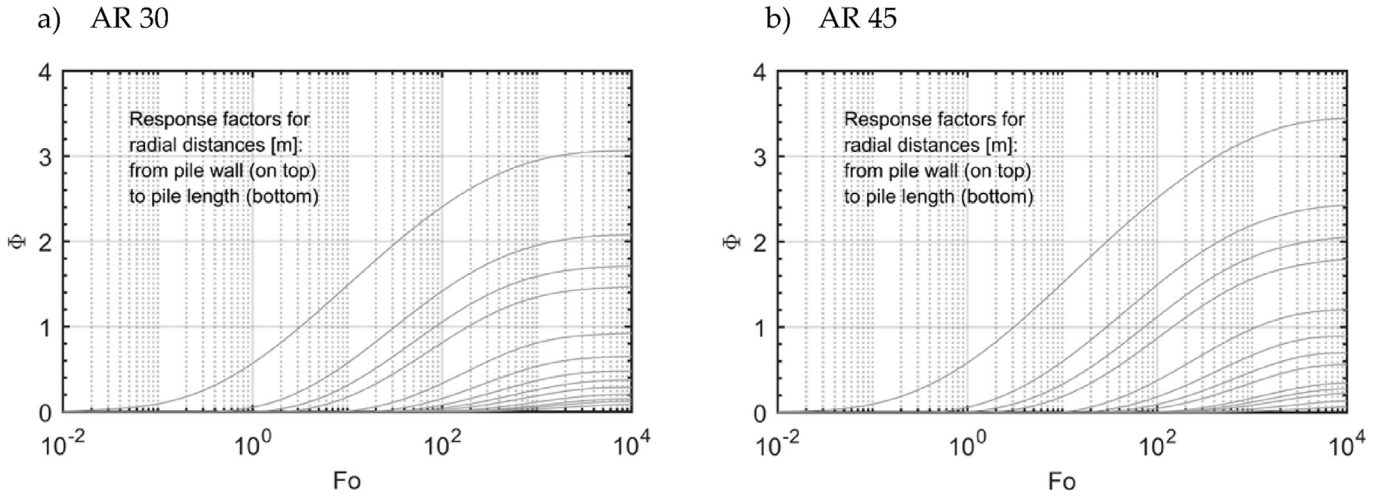

Fig. 14. Dimensionless temperature responses for soil temperature changes at normalised distances $S/2r_b = T_b$, 1.3, 2, 2.6, 5.2, 7.9, 10.5, 13.1, 19.6, 26: a) aspect ratio 30; b) aspect ratio 45 [22].

The inlet and outlet temperatures in the ground loop can be calculated by solving the two-equation system:

The temperatures are fitted with polynomials, to ease implementation. The ground temperature response functions for each distance are valid for min (Fo) < Fo < 10000. For Fo < min (Fo), G_g should be set to zero. G_g can be described as:

$$G_g = a\cdot\ln(Fo)^9 + b\cdot\ln(Fo)^8 + c\cdot\ln(Fo)^7 + d\cdot\ln(Fo)^6 + e\cdot\ln(Fo)^5 + f\cdot\ln(Fo)^4 + g\cdot\ln(Fo)^3 + h\cdot\ln(Fo)^2 + i\cdot\ln(Fo) + j \quad (A.6)$$

The curve fitting parameters are provided below in Tables 3 and 4, for selected radial distances. For intermediate values not considered in the tables of coefficients, a linear interpolation needs to be applied. Linear interpolations are considered sufficient precise and quick [40].

Table 4
Spatial G-function coefficients for AR 45 [22].

$S/2r_b$	∞	1.3	2.6	7.9	10.5	13.1	19.6	45.6
Distance from pile edge [m]	0.00	0.50	1.00	3.00	4.00	5.00	7.50	17.40
a	4.199E-09	2.392E-09	−1.052E-08	−1.870E-09	3.169E-09	5.693E-09	6.248E-09	6.536E-10
b	−3.525E-08	−9.048E-08	7.076E-08	8.660E-08	3.149E-08	−5.976E-09	−4.042E-08	−1.085E-08
c	−8.541E-07	3.281E-07	2.267E-06	1.246E-08	−8.020E-07	−1.156E-06	−1.115E-06	−1.007E-07
d	8.311E-06	1.546E-05	−1.062E-05	−1.446E-05	−6.407E-06	−7.995E-07	4.745E-06	1.493E-06
e	6.477E-05	−8.856E-05	−1.926E-04	2.152E-06	5.308E-05	7.320E-05	6.764E-05	6.226E-06
f	−8.423E-04	−1.116E-03	3.158E-04	7.615E-04	4.225E-04	1.714E-04	−1.086E-04	−5.328E-05
g	−3.519E-03	4.209E-03	7.437E-03	1.341E-03	−2.729E-04	−1.015E-03	−1.256E-03	−1.418E-04
h	4.648E-02	4.981E-02	1.806E-02	−6.134E-03	−4.251E-03	−2.209E-03	5.635E-04	4.997E-04
i	3.245E-01	1.100E-01	4.341E-03	−1.030E-02	−1.528E-03	3.378E-03	6.238E-03	8.745E-04
j	5.817E-01	6.060E-02	−7.559E-03	3.802E-03	4.919E-03	4.112E-03	1.336E-03	−4.694E-04
RMSE[a]	1.658E-05	1.609E-05	1.374E-05	1.943E-05	1.491E-05	9.313E-06	2.111E-06	3.081E-07
R^{2b}	9.999E-01	1.000E+00	1.000E+00	9.998E-01	1.000E+00	9.997E-01	9.971E-01	9.972E-01
min Fo [−]	0.01	0.43	1.7	20	25	32	78	350
min time [h]	0.10	4.36	17.23	202.67	253.34	324.28	790.42	3546.76
max Φ [−]	3.45	2.43	1.79	0.90	0.70	0.56	0.35	0.06
max Fo [−]	10000	10000	10000	10000	10000	10000	10000	10000

[a] RMSE: Root Mean Squared Error.
[b] R^2: Coefficient of Determination.

Table 3
Spatial G-function coefficients for AR 30 [22].

S/2r	∞	1.3	2.6	7.8	10.5	13.1	19.6	31.2
Distance from pile edge [m]	0.00	0.50	1.00	3.00	4.00	5.00	7.50	11.90
a	−6.133E-09	1.592E-08	3.032E-09	−2.950E-08	−1.835E-08	−8.193E-09	4.478E-09	5.694E-09
b	1.568E-07	−3.884E-07	−2.610E-07	6.249E-07	4.464E-07	2.521E-07	−2.753E-08	−9.627E-08
c	−1.134E-06	1.065E-06	3.712E-06	−8.417E-07	−1.408E-06	−1.386E-06	−7.791E-07	−1.265E-07
d	−2.850E-06	3.737E-05	8.788E-06	−4.916E-05	−3.272E-05	−1.717E-05	3.368E-06	7.355E-06
e	1.151E-04	−1.932E-04	−3.290E-04	1.488E-04	1.576E-04	1.253E-04	4.287E-05	−7.582E-06
f	−7.257E-04	−1.620E-03	1.088E-05	1.312E-03	8.230E-04	4.161E-04	−7.755E-05	−1.598E-04
g	−4.868E-03	6.314E-03	9.692E-03	−2.005E-03	−2.544E-03	−2.093E-03	−6.775E-04	1.941E-04
h	4.514E-02	5.190E-02	1.794E-02	−8.278E-03	−5.495E-03	−2.838E-03	4.586E-04	9.959E-04
i	3.243E-01	9.452E-02	−5.962E-03	6.321E-03	8.970E-03	7.734E-03	2.646E-03	−7.663E-04
j	5.689E-01	5.337E-02	−8.649E-03	7.817E-03	6.984E-03	4.715E-03	5.910E-04	−9.730E-04
RMSE[a]	1.138E-05	9.286E-06	8.402E-06	5.272E-06	5.359E-06	5.164E-06	1.858E-06	1.107E-07
R^{2b}	1.000E+00	9.997E-01	9.999E-01	9.999E-01	1.000E+00	1.000E+00	1.000E+00	9.998E-01
min Fo [−]	0.01	0.43	2.10	20.00	26.00	33.50	58.00	175.00
min time [h]	0.10	4.36	21.28	202.67	263.47	339.48	587.75	1773.38
max Φ [−]	3.07	2.07	1.46	0.65	0.48	0.37	0.21	0.09
max Fo [−]	10000	10000	10000	10000	10000	10000	10000	10000

[a] RMSE: Root Mean Squared Error.
[b] R^2: Coefficient of Determination.

The curves provided in Fig. 14 and described by Equation (A.6) can be superimposed in time and space to account for multiple piles. This principle relies on the heat conduction equation and boundary conditions on being linear [41]. In the spatial superposition the temperature distributions around every ground heat exchanger are added in order to calculate the overall temperature variation at the pile walls [42]:

$$\Delta T_b(t) = \frac{1}{n_p}\sum_{i=1}^{n_p}\sum_{j=1}^{n_p}\overline{\Delta T_b}(d_{ij}, t) \quad (A.7)$$

$$d_{ij} = \begin{cases} r_b, & i = j \\ \sqrt{(x_i - x_j)^2 + (y_i - y_j)^2}, & i \neq j \end{cases} \quad (A.8)$$

where ΔT_b [K] is the average temperature variation at the pile heat exchanger wall, (x_i, y_i) [m] are the coordinates of the ith pile heat exchanger, n_p is the number of pile heat exchangers in the foundation and d_{ij} [m] is the pile distance.

Time variations can be applied by deconvolution of the time varying heat transfer rate [41]. The temperature at discrete time step in the pile heat exchanger foundation is computed as:

Please cite this article in press as: M. Alberdi-Pagola, et al., A case study of the sizing and optimisation of an energy pile foundation (Rosborg, Denmark), Renewable Energy (2018), https://doi.org/10.1016/j.renene.2018.07.100

$$\Delta T_n = \sum_{i=1}^{i=n} \frac{q_i}{2\pi\lambda_s}\left(G\left(Fo_n - Fo_{(i-1)}\right) - G(Fo_n - Fo_i)\right) \quad (A.9)$$

where n is the point in normalised time in which the superposition is evaluated.

The steady state concrete thermal resistance R_c [K·m/W] and the concrete G-function for the transient response of the pile G_c [39,43] depend on the shape of the pile cross section, the position of the pipes and the ratio between the thermal conductivity of the concrete and the soil. The transient response of the pile concrete is calculated as the proportion of the steady state thermal resistance that has been achieved in the 3D FEM simulations at a given value of time Fo:

$$R_c = \frac{T_p - T_b}{q} \quad (A.10)$$

where T_p [°C] is the average temperature on the outer wall of the pipe.

Alberdi-Pagola et al. [33] provided the pile thermal resistance for different ratios between soil and concrete thermal conductivity, λ_c/λ_s (Fig. 15a). The temporal development in the proportion of steady state pile thermal resistance R_c for W-shape pipe arrangements is shown in Fig. 15b for ratios $\lambda_c/\lambda_s = 0.5$, 1 and 2 [20].

non-computed values.

Table 5
Curve fitting parameters for upper and lower bounds for the concrete thermal resistance R_c [22].

λ_c/λ_s	W-shape	
	2	0.5
a	−0.00105	−0.00096
b	0.01557	0.01422
c	−0.09284	−0.08438
d	0.28459	0.25660
e	−0.47303	−0.42066
f	0.40727	0.35237

Table 6
Curve fitting parameters for concrete G-functions G_c [22].

λ_c/λ_s	2U		
	0.5	1	2
a	7.4143E-07	3.2209E-06	−6.8329E-07
b	−1.6587E-05	3.5142E-05	1.2454E-05
c	6.6686E-05	−2.3294E-04	−4.7563E-05
d	1.0464E-03	−1.0900E-04	3.1674E-05
e	−1.2676E-02	−5.0508E-03	−4.8439E-03
f	5.8398E-02	5.3798E-02	4.9111E-02
g	8.8640E-01	8.6614E-01	8.6694E-01
RMSE[a]	0.0039	0.0025	0.00003
R^2[b]	0.9991	0.9997	0.99992

[a] RMSE: Root Mean Squared Error.
[b] R^2: Coefficient of Determination.

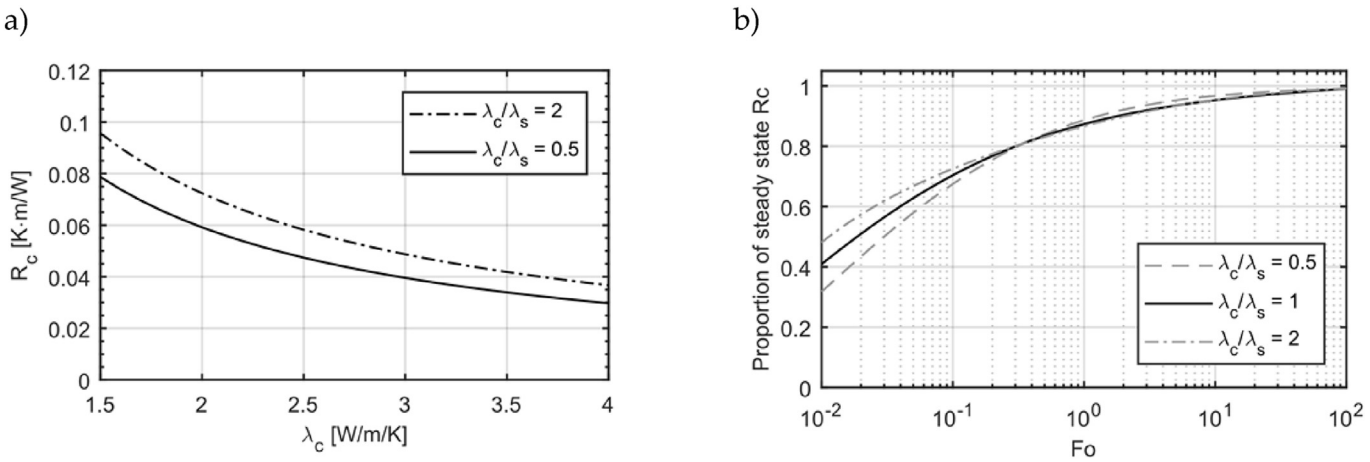

Fig. 15. a) 3D model estimated upper and lower bounds for the concrete thermal resistance Rc [33]. b) Proportion of steady state Rc [20]. Both subplots correspond to W-shape pipe arrangements.

The curves are fitted with polynomials, to ease implementation. The upper and lower bounds for the concrete thermal resistance R_c for square precast pile heat exchangers with W-shape pipes for a range of thermal conductivities of concrete ($1 < \lambda_c < 4$) take the form of Equation (A.11), while the concrete temperature response G-function G_c, valid for $0.01 < Fo < 100$, takes the form of Equation (A.12):

$$R_c = a\cdot\lambda_c^5 + b\cdot\lambda_c^4 + c\cdot\lambda_c^3 + d\cdot\lambda_c^2 + e\cdot\lambda_c + f \quad (A.11)$$

$$G_c = a\cdot\ln(Fo)^6 + b\cdot\ln(Fo)^5 + c\cdot\ln(Fo)^4 + d\cdot\ln(Fo)^3 + e\cdot\ln(Fo)^2 + f\cdot\ln(Fo) + g \quad (A.12)$$

The curve fitting parameters for R_c and R_c are defined in Tables 5 and 6, respectively. As before, linear interpolation is suggested for

The pipe thermal resistance R_{pipe} [K·m/W] is defined in Equation (A.13) as the sum of the pipe convective (first term on right hand side) and conductive (second term on right hand side) resistances:

$$R_{pipe} = \frac{1}{2n\pi r_i h_i} + \frac{\ln(r_o/r_i)}{2n\pi\lambda_{pipe}} \quad (A.13)$$

where n is the number of pipes in the pile heat exchanger cross section, r_i [m] is the inner radius of the pipe, r_o [m] is the outer radius of the pipe, h_i [W/m^2/K] is the heat transfer coefficient and λ_{pipe} [W/m/K] is the thermal conductivity of the pipe material. h_i can be calculated using the Gnielinski correlation as described in Refs. [44,45].

Please cite this article in press as: M. Alberdi-Pagola, et al., A case study of the sizing and optimisation of an energy pile foundation (Rosborg, Denmark), Renewable Energy (2018), https://doi.org/10.1016/j.renene.2018.07.100

References

[1] S.J. Rees, An introduction to ground-source heat pump technology, in: Adv. Ground-source Heat Pump Syst, Woodhead Publishing, 2016, pp. 1–25. https://doi.org/10.1016/B978-0-08-100311-4.00001-7.
[2] J.W. Lund, T.L. Boyd, Direct utilization of geothermal energy 2015 worldwide review, Geothermics 60 (2016) 66–93. https://doi.org/10.1016/j.geothermics.2015.11.004.
[3] H. Brandl, Energy foundations and other thermo-active ground structures, Geotechnique 56 (2006) 81–122. https://doi.org/10.1680/geot.2006.56.2.81.
[4] L. Laloui, A. Di Donna, Energy Geostructures: Innovation in Underground Engineering, John Wiley & Sons, Inc., 2013, ISBN 978-1-84821-572-6.
[5] A. Di Donna, B. Marco, A. Tony, Energy Geostructures: analysis from research and systems installed around the World, in: DFI 2017: 42nd Annual Conference on Deep Foundations, USA, 2017.
[6] D. Nicholson, P. Smith, G.A. Bowers, F. Cuceoglu, C.G. Olgun, J.S. McCartney, K. Henry, L.L. Meyer, F.A. Loveridge, Environmental impact calculations, life cycle cost analysis, DFI J. J. Deep Found. Inst. 8 (2014) 130–146, https://doi.org/10.1179/1937525514Y.0000000009.
[7] J. Gao, A. Li, X. Xu, W. Gang, T. Yan, Ground heat exchangers: applications, technology integration and potentials for zero energy buildings, Renew. Energy 128 (2018) 337–349, https://doi.org/10.1016/J.RENENE.2018.05.089.
[8] J.D. Spitler, GLHEPRO-A design tool for commercial building ground loop heat exchangers, in: Proc. Fourth Int. Heat Pumps Cold Clim. Conf., Citeseer, 2000.
[9] Building Physics, Earth Energy Designer EED 4, 2017. https://www.buildingphysics.com/manuals/EED4.pdf.
[10] Geo Connections, Loop Link PRO, 2018. https://looplinkpro.com/features/.
[11] Gaia Geothermal, GLD Overview, 2016. http://www.gaiageo.com/products.html.
[12] M. de Paly, J. Hecht-Méndez, M. Beck, P. Blum, A. Zell, P. Bayer, Optimization of energy extraction for closed shallow geothermal systems using linear programming, Geothermics 43 (2012) 57–65. https://doi.org/10.1016/j.geothermics.2012.03.001.
[13] M. Beck, P. Bayer, M. de Paly, J. Hecht-Méndez, A. Zell, Geometric arrangement and operation mode adjustment in low-enthalpy geothermal borehole fields for heating, Energy 49 (2013) 434–443. https://doi.org/10.1016/j.energy.2012.10.060.
[14] C. Maragna, Development of a numerical platform for the optimization of borehole heat exchanger fields, Eur. Geotherm. Congr. 2016 (2016) 19–24.
[15] J. Fadejev, R. Simson, J. Kurnitski, F. Haghighat, A review on energy piles design, sizing and modelling, Energy 122 (2017) 390–407, https://doi.org/10.1016/j.energy.2017.01.097.
[16] H. Bjorn, Shallow geothermal energy from a Danish standpoint, Geoth. Energy (2018) (press note).
[17] D. Pahud, A. Fromentin, D. ambiente costruzioni e design I. sostenibilità applicata all'ambiente costruito, PILESIM - LASEN. Simulation Tool for Heating/Cooling Systems with Heat Exchanger Piles or Borehole Heat Exchangers, User Manual, 1999. http://repository.supsi.ch/id/eprint/3047.
[18] N. Makasis, G.A. Narsilio, A. Bidarmaghz, A machine learning approach to energy pile design, Comput. Geotech. 97 (2018) 189–203, https://doi.org/10.1016/J.COMPGEO.2018.01.011.
[19] F. Loveridge, W. Powrie, G-Functions for multiple interacting pile heat exchangers, Energy 64 (2014) 747–757. https://doi.org/10.1016/j.energy.2013.11.014.
[20] M. Alberdi-Pagola, S. E. Poulsen, R. L. Jensen, S. Madsen, Design methodology for precast quadratic pile heat exchanger-based shallow geothermal ground-loops: multiple pile g-functions, Geothermics. (under review).
[21] G. Derringer, R. Suich, Simultaneous optimization of several response variables, J. Qual. Technol. 12 (1980) 214–219, https://doi.org/10.1080/00224065.1980.11980968.
[22] M. Alberdi-Pagola, R.L. Jensen, S. Madsen, S.E. Poulsen, Method to Obtain G-functions for Multiple Precast Quadratic Pile Heat Exchangers, Aalborg University, Aalborg, Denmark, 2018. http://vbn.aau.dk/files/274763046/Method_to_obtain_g_functions_for_multiple_precast_quadratic_pile_heat_exchangers.pdf.
[23] P. Eskilson, Thermal Analysis of Heat Extraction, PhD thesis, University of Lund, Sweden, 1987.
[24] F. Dupray, L. Laloui, A. Kazangba, Numerical analysis of seasonal heat storage in an energy pile foundation, Comput. Geotech. 55 (2014) 67–77. https://doi.org/10.1016/j.compgeo.2013.08.004.
[25] The MathWorks Inc, MATLAB R2017a and Global Optimization Toolbox, 2017.
[26] N.R. Costa, J. Lourenço, Z.L. Pereira, Desirability function approach: a review and performance evaluation in adverse conditions, Chemometr. Intell. Lab. Syst. 107 (2011) 234–244, https://doi.org/10.1016/J.CHEMOLAB.2011.04.004.
[27] Nist Sematech, Engineering Statistics Handbook. Multiple Responses: the Desirability Approach, 2013. https://www.itl.nist.gov/div898/handbook/pri/section5/pri5322.htm. (Accessed 11 May 2018).
[28] VDI, VDI 4640 Thermal Use of the Underground. Part 2: Ground Source Heat Pump Systems, The Association of German Engineers (VDI), 2001.
[29] O. Møller, J.K. Frederiksen, A.H. Augustesen, N. Okkels, K.G. Sorensen, Design of piles – Danish practice, in: Proceedings of ISSMGE - ETC 3 International Symposium on Design of Piles in Europe, 2016.
[30] Centrum Pæle A/S, Personal Communication, 2018.
[31] M. Alberdi-Pagola, R.L. Jensen, S.E. Poulsen, A performance case study of energy pile foundation at Rosborg Gymnasium (Denmark), in: 12th REHVA World Congr. Clima 2016, Department of Civil Engineering, Aalborg University, Aalborg, Denmark, 2016, p. 10. http://vbn.aau.dk/files/233716932/paper_472.pdf.
[32] M. Alberdi-Pagola, R.L. Jensen, S. Madsen, S.E. Poulsen, Measurement of Thermal Properties of Soil and Concrete Samples, Aalborg University, Aalborg, Denmark, 2017. http://vbn.aau.dk/files/266378485/Measurement_of_thermal_properties_of_soil_and_concrete_samples.pdf.
[33] M. Alberdi -Pagola, S.E. Poulsen, F. Loveridge, S. Madsen, R.L. Jensen, Comparing heat flow models for interpretation of precast quadratic pile heat exchanger thermal response tests, Energy 145 (2018) 721–733, https://doi.org/10.1016/j.energy.2017.12.104.
[34] F. Cecinato, F.A. Loveridge, Influences on the thermal efficiency of energy piles, Energy 82 (2015) 1021–1033. https://doi.org/10.1016/j.energy.2015.02.001.
[35] M. Faizal, A. Bouazza, R.M. Singh, Heat transfer enhancement of geothermal energy piles, Renew. Sustain. Energy Rev. 57 (2016) 16–33. https://doi.org/10.1016/j.rser.2015.12.065.
[36] S. Gehlin, Thermal Response Test. Method Development and Evaluation, PhD thesis, Luleå University of Technology, 2002.
[37] M. Global, Ethylene Glycol Product Guide, 2008. http://www.meglobal.biz/media/product_guides/MEGlobal_MEG.pdf.
[38] Engineering Toolbox, Ethylene Glycol Heat-transfer Fluid, 2003. https://www.engineeringtoolbox.com/ethylene-glycol-d_146.html. (Accessed 30 March 2018).
[39] F. Loveridge, W. Powrie, Temperature response functions (G-functions) for single pile heat exchangers, Energy 57 (2013) 554–564. https://doi.org/10.1016/j.energy.2013.04.060.
[40] E. Zanchini, S. Lazzari, Temperature distribution in a field of long Borehole Heat Exchangers (BHEs) subjected to a monthly averaged heat flux, Energy 59 (2013) 570–580. https://doi.org/10.1016/j.energy.2013.06.040.
[41] J.D. Spitler, M. Bernier, 2 - Vertical borehole ground heat exchanger design methods, in: S.J. Rees (Ed.), Adv. Ground-source Heat Pump Syst, Woodhead Publishing, 2016, pp. 29–61. https://doi.org/10.1016/B978-0-08-100311-4.00002-9.
[42] M. Cimmino, M. Bernier, F. Adams, A contribution towards the determination of g-functions using the finite line source, Appl. Therm. Eng. 51 (2013) 401–412. https://doi.org/10.1016/j.applthermaleng.2012.07.044.
[43] F. Loveridge, W. Powrie, 2D thermal resistance of pile heat exchangers, Geothermics 50 (2014) 122–135. https://doi.org/10.1016/j.geothermics.2013.09.015.
[44] R. Al-Khoury, Computational Modeling of Shallow Geothermal Systems, CRC Press, 2011.
[45] H.-J.G. Diersch, FEFLOW Finite Element Modeling of Flow, Mass and Heat Transport in Porous and Fractured Media, Springer Science & Business Media, 2014, https://doi.org/10.1007/978-3-642-38739-5.

Please cite this article in press as: M. Alberdi-Pagola, et al., A case study of the sizing and optimisation of an energy pile foundation (Rosborg, Denmark), Renewable Energy (2018), https://doi.org/10.1016/j.renene.2018.07.100